High Temperature Strength and Fractographic Study of Sialon

A.K. Mukhopadhyay and D. Chakraborty
Central Glass and Ceramic Research Institute, P.O. Jadavpur University, Calcutta – 700 032, India

CONTENTS

ABSTRACT

High temperature (30-1400°C) strength, Young's modulus and fracture toughness, K_{1C} (SENB) data are reported for reaction sintered sialon having three different compositions and for three different compositions of liquid phase sintered sialon. The influence of composition, microstructure, defect type, density and slow crack growth on the aforesaid mechanical properties are discussed. Attention is focused on the interdependence of strength, Young's modulus and fracture toughness. Fractographically predicted strength matched excellently with experimentally measured strength at different temperatures of the sialon products.

1. INTRODUCTION

'Sialon' is an acronym for the solid solution of aluminium oxide in silicon nitride (Si_3N_4). During the last two decades sialon has shown great promise as structural as well as cutting tool ceramics /1-5/.

Reaction sintered sialon of different compositions show constant strength up to 1200°C /1-3/. Increases in milling time of the powder mixture and amount of alumina present in excess of the stoichiometric composition are reported to have a beneficial influence on strength in the temperature range 30-1400°C of these materials

/2-4/. Use of Y_2O_3 as a sintering aid, reduction in substitution level, increase in amount of Y_2O_3-SiO_2 sintering additive and enrichment of grain boundary phase in yttrium alumina garnet content have been found to improve high temperature strength of liquid phase sintered sialon /5-8/. Strength above 1200°C of both types of sialon degrade due to slow crack growth /1, 6/. Limited study on ambient Young's moduli of both types of sialon indicates an increasing trend with density /1, 9/. Cavities and surface flaws are known to act as fracture sources in reaction sintered sialon under ambient conditions /10/.

The purpose of the present work was (i) to study high temperature 30-1400°C) strength and Young's moduli of reaction sintered and liquid phase sintered sialon, (ii) to determine the dependence of strength on Young's moduli and fracture toughness of these materials and (iii) to compare fractographically predicted strength with experimentally measured strength of the different sialon products in the temperature range 30-1200°C.

2. EXPERIMENTAL

2.1. Materials

In the general formula $Si_{6-Z}Al_ZO_ZN_{8-Z}$ for the solid solution of aluminium oxide in silicon nitride, Z represents the number of oxygen atoms replacing nitrogen. Si_3N_4 powder (99.4% purity, α:β=86:14) prepared in the laboratory /11/ by nitridation of Si was the principal raw material for preparation of reaction sintered sialon A(Z=1), B(Z=1) and C(Z=0.5) and liquid phase sintered sialon D(Z=0.5), E(Z=0.5) and F(Z=0.5). Table 1 gives an analysis of the starting materials, Si and Si_3N_4, carried out by conventional methods.

The other components were AlN (A grade, Starck, West Germany), Al_2O_3 (98% purity, Sarabhai M. Chemicals, India), Y_2O_3 (99.99% purity, Indian Rare Earth Limited, India), MgO (GR grade, E. Merck, G.D.R.) and SiO_2 (99% purity, optical grade, India). Table 2 shows wt.% of different components, wt.% of liquid phase and Z values in starting batch compositions of reaction sintered sialon A, B and C synthesised from the Si_3N_4-AlN-Al_2O_3 system and liquid phase sintered sialon D, E and F synthesised from the Y_2O_3-AlN-SiO_2 and MgO-SiO_2 systems. The milled powder was cold compacted isostatically to billets. Sintering of the green billets was performed in a BN coated graphite crucible for 30-90 mins. in a pure nitrogen atmosphere at 1700-1800°C using a graphite resistance furnace (Astro, USA). To prevent thermal deposition and evaporational weight loss at the sintering temperature, the green billets were tightly embedded in a packing material of Si_3N_4:SiO_2 in the ratio 70:30 inside the BN coated graphite crucible. Depending on sintering temperature, weight loss of reaction sintered sialon varied in the range 0-1.21% and that of liquid phase sintered sialon varied in the range 0-0.23% /12-13/.

TABLE 1

Analysis of Raw Materials

Component	Silicon (Wt.%)	Silicon Nitride (Wt.%)
Si	99.40	-
N	-	38.63±0.51
O	-	2.20±0.30
Ca	0.0048	0.053
Mg	0.02	0.01
K	0.02	-
Na	0.069	0.083
P	0.016	-
S	0.01	-
C	0.05	-
Fe	0.28	-

- not determined

TABLE 2

Composition of reaction sintered sialon (A, B and C) and liquid phase sintered sialon (D, E and F)

Material Type	Composition (wt.%)						Z	Liquid Phase (wt.%)
	Si_3N_4	Al_2O_3	AlN	MgO	Y_2O_3	SiO_2		
Reaction Sintered Sialon								
A	83.02	7.39	9.59	-	-	-	1.0	-
B	83.42	9.55	7.04	-	-	-	1.0	-
C	91.73	3.85	4.40	-	-	-	0.5	-
Liquid Phase Sintered Sialon								
D	88.37	4.50	5.33	-	1.77	-	0.5	5
E	79.93	5.42	7.57	-	5.46	1.62	0.5	15
F	86.94	5.75	2.31	5.0	-	-	0.5	8

- not present in starting composition

Phase identification of the sintered products was performed by XRD (Phillips PW1730, Holland). β' sialon was the major phase in both types of sialon. Density of various sialon products was measured by Archimedes principle. Estimation of grain size was carried out by SEM (Cambridge, Stereoscan 5250, UK) examination of fractured as well as polished and etched surfaces. Etching was performed in molten NaOH at 350°C for 30-90 secs. Table 3 contains the data on grain size distribution parameters, aspect ratio of elongated grains and fired density of different sialon products.

2.2. Methods

High temperature (30-1400°C) strength, Young's modulus and fracture toughness, K_{1C} (SENB) of ground and polished sialon samples (45x4.5x3.5 mm^3) were

TABLE 3

Grain size parameters and density of different sialon materials

Sialon Type	Grain Size		Aspect Ratio	Density
	Average length $\bar{l}$ (μm)	Average breadth $\bar{b}$ (μm)	$(\bar{l}/\bar{b})$	(gcc^{-1})
A	2.78±0.85	0.89+0.32	3.12	3.09
B	-	-	-	2.51
C	-	-	-	2.42
D	1.84+0.76	0.51+0.16	3.61	3.09
E	1.91+0.37	0.59+0.13	3.24	2.98
F	2.01+0.31	0.64+0.15	3.14	2.94

measured by four point bending using a High Temperature Bending Strength Tester (model 422S, Netzsch, West Germany). The following equations were used for calculations of strength (σ) and Young's modulus (E)

$$\sigma = 3P_f d/BW^2 \quad (1)$$

$$E = P_f d(3L^2 - 4d^2)/4yBW^3 \quad (2)$$

where P_f is load at fracture, d is bending arm (10.04 mm), B and W are sample breadth and width respectively, L is major span (40.10 mm) and y is deflection of central point of sample with respect to outer loading points /14-15/. Details of fracture toughness testing have been published elsewhere /16/. In all experiments a loading rate of 1.25N/min was used. An average of 4-6 observations was taken as representative data.

The following equation was used for calculation of predicted strength (σ_p)

$$\sigma_p = (Z/Y)\ (K_{1C})/(a_c)^{1/2} \quad (3)$$

where Z is a flaw shape parameter, a dimensionless factor which depends on the flaw depth/flaw width ratio, Y is another dimensionless factor which depends on flaw depth and test geometry, and a_c is the critical flaw size measured from SEM photographs of fracture surfaces. Further details of the fractography may be found elsewhere /17/.

3. RESULTS AND DISCUSSION

The temperature dependence of strength and Young's moduli for reaction sintered sialon samples A, B and C and liquid phase sintered sialon samples D, E and F are discussed separately below.

3.1. Strength of reaction sintered sialon samples (A, B and C); influence of temperature, density, slow crack growth and composition.

Figure 1 shows that comparing C, B and A, the last one has the highest values of strength in the temperature range 30-1400°C. Strength at 1200°C of sialon A slightly increased over strength at 30°C but the strength of B was constant in a similar temperature range. At 1400°C, strength of sialon A degraded by 17% while that of sialon B at the same temperature increased by 19% compared to their respective strength values under ambient condition.

In spite of having a lower density than sialon B, sialon C had strength values at 30 and 1200°C considerably higher than sialon B (Table 3 and Figure 1).

Since both the reaction sintered sialon products A and B have similar Z values (Z=1, Table 2), the superior strength characteristics of A (Figure 1) may be attributed to its higher density (Table 3). Strength data in the temperature range 30-1200°C of A were comparable to values reported for reaction sintered sialon by Wills et al /1/ but strength at 1400°C of A was far superior to data reported by the same workers. Marked non-linearity was noted in the load versus deflection curve of A at 1400°C (Figure 2). This indicates the plastic flow of material at 1400°C of A even though no liquid phase was added in the starting composition (Table 2). Fractographic observation (Figure 3) confirmed the region of slow crack growth on typical fracture surface at 1400°C of A. Wills et at /1/ have also reported similar phenomena at a similar temperature for reaction sintered sialon.

Slight increase in strength at 1400°C of sialon B may be due to oxidation induced healing of surface cracks and filling up of internal voids by the oxidation products. Since sintering time and temperature were identical for the sialon materials B and C /12/, the superior strength characteristics

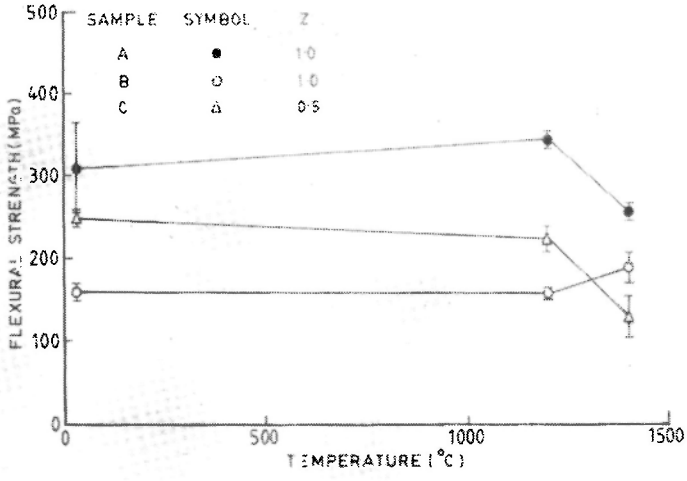

Fig. 1 High temperature strength of reaction sintered sialon A, B and C.

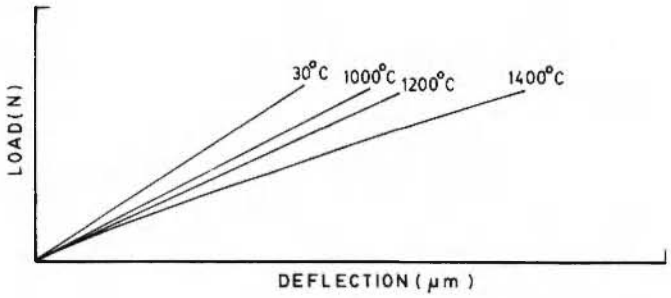

Fig. 2 Typical load-deflection behaviour in the temperature range 30-1400°C of the sialon A.

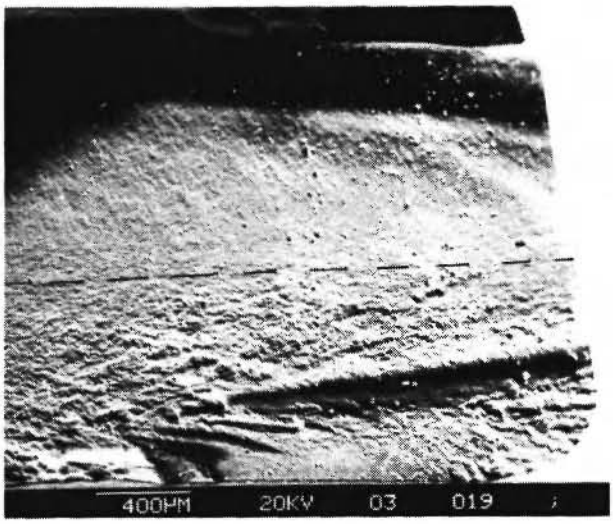

Fig. 3 Slow crack growth at 1400°C of the sialon A (dashed lines mark the boundary between slow crack growth and fast crack propagation region).

of C compared to B in the temperature range 30-1200°C (Figure 1) may be attributed to its lower Z value (Table 2). However, the reason why this beneficial influence of reduction in Z value did not hold good at 1400°C (Figure 1) is yet to be understood. In the case of liquid phase sintered sialon, beneficial influence of reduction in Z value on high temperature strength has been reported by other workers /7/.

3.2. Strength of liquid phase sintered sialon (D and F); influence of temperature, microstructure, composition and defect type.

Figure 4 shows that in the temperature range 30-1000°C of sialon D, strength was nearly constant and at 1200°C there was about 40% degradation in strength with respect to the ambient value. On the contrary, strength in the temperature range 30-1200°C of sialon F exhibits a steadily decreasing trend and at 1200°C strength degraded by 66% over the ambient value. Further, in the temperature range 30-1200°C, the strength of liquid phase sintered sialon D, synthesised with 5 wt.% of nitrogen rich liquid from the Y_2O_3-AlN-SiO_2 system, was far superior to liquid phase sintered sialon F, synthesised with 8 wt.% of conventional silicate rich liquid from the MgO-SiO_2 system (Table 2 and Figure 4).

At 30°C the higher strength of the sialon D compared to F may be linked to its smaller grain size (Table 3). Based on starting composition (Table 2) one would expect the formation of a yttrium sialon and a magnesium sialon glassy phase at the grain boundaries of D and F, respectively. In the temperature range 800-1100°C viscosity of yttrium sialon glass has been found to be higher than magnesium sialon glass /18/. Therefore, the grain boundary oxynitride glassy phase of D was most likely more refractory than the glassy phase in F. Consequently, high temperature strength of sialon D

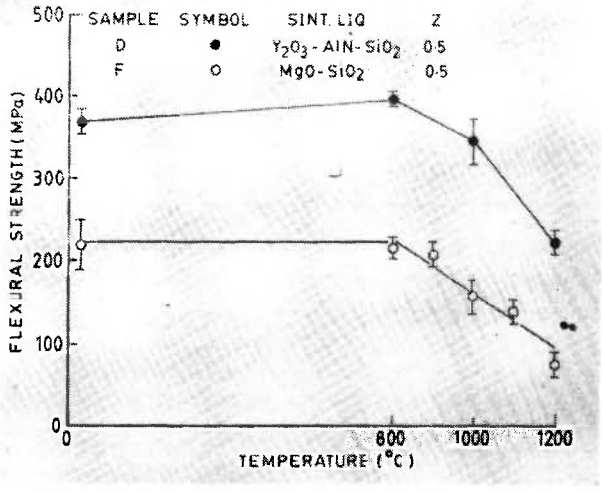

Fig. 4 High temperature strength of liquid phase sintered sialon D and F.

was far superior to that in F. The cause of the significant degradation in strength above 1000°C of both of these sialon products, D and F, is discussed later in this paper.

Fractographic study identified sub-surface voids (Figure 5) and grinding induced surface damage (Figure 6) as the most typical fracture origins at 30°C of the sialon products D and F, respectively /17/. Since in four point flexural loading the tensile surface is under maximum stress, the presence of surface failure origin leads more to characteristically lower strength than that caused by sub-surface failure origin. This observation helps one to understand why ambient strength of sialon F was much lower than that of sialon D. Lower strength at 30°C of sialon F could also be attributed partially to its predominantly transgranular mode of fracture (Figure 7).

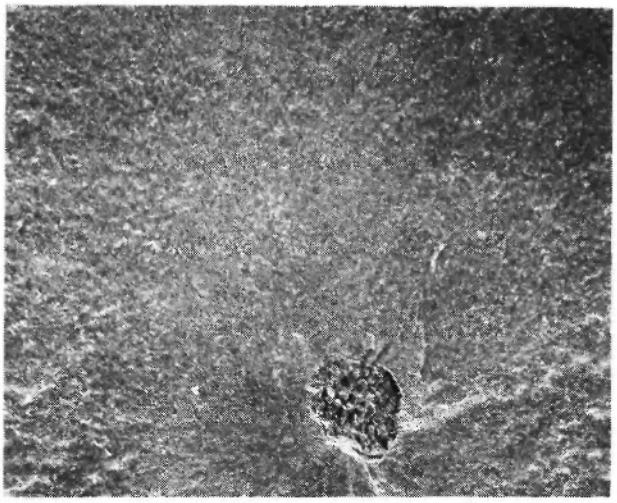

Fig. 5 Sub-surface fracture origin at 30°C of the sialon D (bar = 10μm).

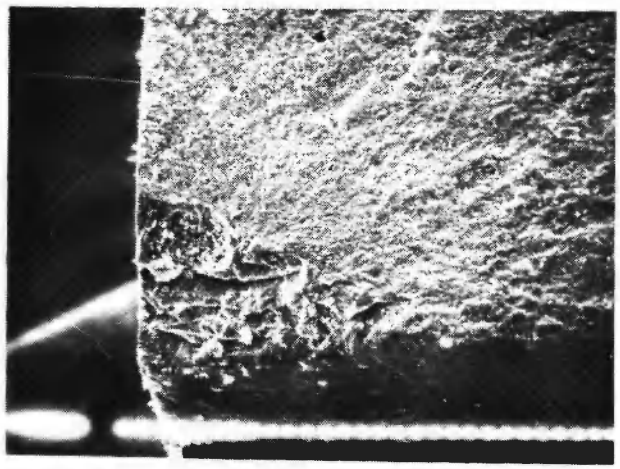

Fig. 6 Surface fracture origin at 30°C of the sialon F (bar = 10μm).

3.3. *Young's moduli of reaction sintered sialon samples (A, B and C); influence of temperature and density.*

Figure 8 shows Young's moduli in the temperature range 30-1400°C of reaction sintered sialon samples A, B and C. The Young's moduli of all the three sialon samples degraded with increase in temperature. Out of C, B and A, the last one had the highest values of Young's moduli in the aforementioned range of temperatures. At 1000, 1200 and 1400°C of both the sialon samples A and B, the extent of percentage degradation in Young's moduli with respect to their respective values at 30°C were nearly similar. Young's moduli at 1200 and 1400°C of the sialon C degraded by 39% and 97% respectively over the Young's modulus measured at 30°C. These were the highest values of percentage degradation of

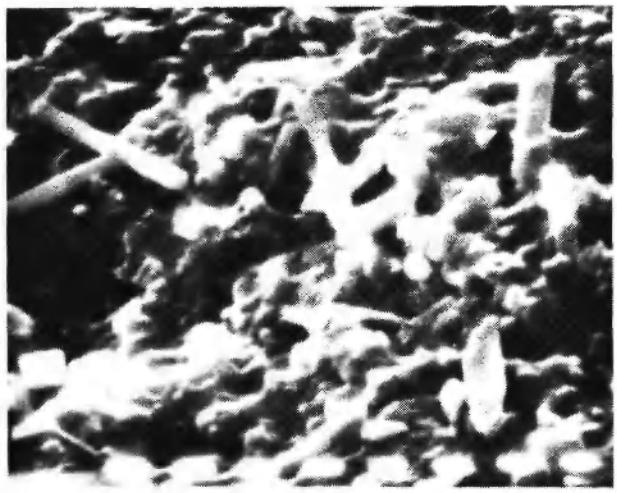

Fig. 7 Predominantly transgranular mode of fracture at 30°C of the sialon F (bar = 10μm).

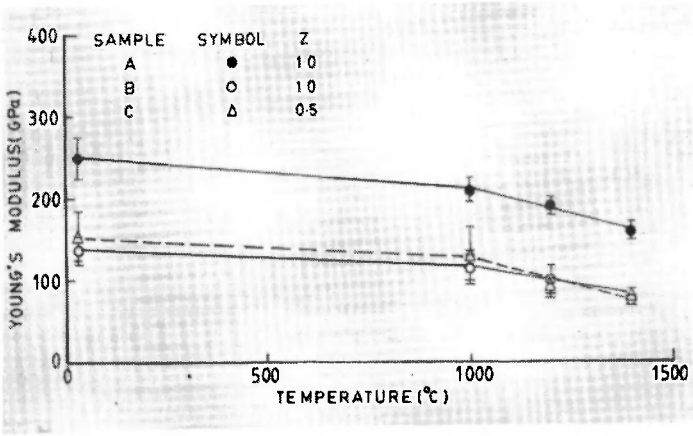

Fig. 8 High temperature Young's moduli of reaction sintered sialon A, B and C.

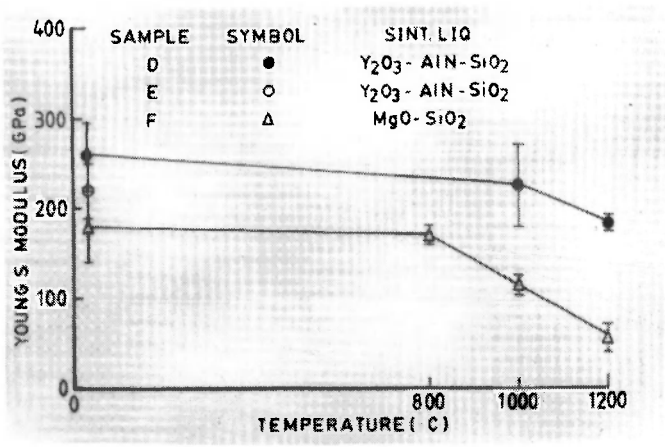

Fig. 9 High temperature Young's moduli of liquid phase sintered sialon D, E and F.

Young's moduli at 1200 and 1400°C of the reaction sintered sialon samples used in the present work. Since both the sialon products A and B had similar values of Z (=1) in their respective starting compositions (Table 2), the higher Young's moduli of A than B may be attributed to higher density of A (Table 3). Other workers also have reported an increasing trend of Young's modulus with higher density of reaction sintered sialon /1/.

3.4. Young's moduli of liquid phase sintered sialon samples (D, E and F); influence of temperature, microstructure and composition.

Figure 9 shows Young's moduli in the temperature range 30-1200°C of the liquid phase sintered sialon samples D, E and F. The Young's moduli of both D and F decreased with increase in temperature. Out of F, E and D, the last one had the highest and the first the lowest values of Young's moduli in the aforementioned range of temperature. At 30°C, Young's modulus of sialon E was intermediate to those of D and F. With respect to ambient value, the percentage degradations in Young's moduli at 1000 and 1200°C of F was much higher than those of sialon E.

Under ambient condition, Young's moduli of the liquid phase sintered sialon samples D, E and F increased with decrease in average grain size and increase in aspect ratio of elongated grains in the microstructure (Table 3 and Figure 9).

The sialon products D and E were prepared with 5 and 15 wt.% of sintering liquid, respectively, from the Y_2O_3-AlN-SiO_2 system (Table 2). For the given Y_2O_3-AlN-SiO_2 system, clearly the increase in wt.% of sintering liquid had a deleterious effect on improvement of Young's modulus at 30°C (Figure 9). The superior Young's modulus characteristics in the temperature range 30-1200°C of sialon D in comparison to sialon F may be discussed in terms of the difference in their respective starting compositions (Table 2) in a similar fashion as used earlier in explaining the temperature dependencies of their strength characteristics (Sub-section 3.2).

3.5. Dependence of strength on Young's modulus and fracture toughness.

Figure 10 reveals that for both the reaction sintered sialon samples (A, B and C) and the liquid phase sintered sialon samples (D, E and F) an improvement or degradation in strength values were generally associated with a corresponding improvement or degradation in respective Young's moduli values. This was true at both 30 and 1200°C. In the cases of both reaction bonded and liquid phase sintered silicon nitrides we have previously observed /14, 19/ the occurrence of similar phenomena.

Figure 11 shows that at both 30 and 1200°C, an improvement or degradation in strength values of both the reaction sintered sialon samples (A and B) and the liquid phase sintered sialon samples (D and F) were generally associated also with a

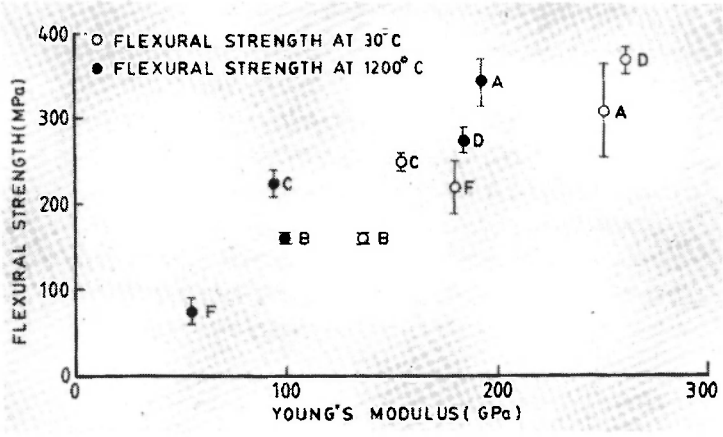

Fig. 10 Interdependence of strength and Young's moduli for reaction sintered and liquid phase sintered sialon materials.

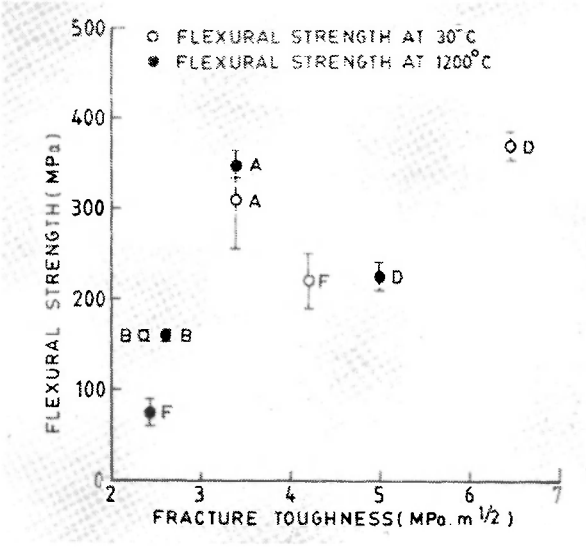

Fig. 11 Dependence of strength on fracture toughness of reaction sintered and liquid phase sintered sialon materials.

corresponding improvement or degradation in their respective fracture toughness, K_{1C} (SENB), values /16/. We have reported the occurrence of similar phenomena in the cases of both reaction bonded and liquid phase sintered silicon nitrides /14, 19/. At ambient temperature, a similar correspondence of Young's modulus, fracture toughness and strength has also been noted in the case of fibrous silica /20/.

The general trend of degradation in K_{1C} at 1200°C of both D and F (Figure 11) explains in particular the significant decrease in their respective strength values at the same temperature. We have previously observed that the degradation in K_{1C} at 1200°C of liquid phase sintered sialon is due to the occurrence of variations in the extent of slow crack growth dependent upon composition /16/.

3.6. *Fractography*

Table 4 shows the comparison between fractographically predicted strength and experimentally measured strength at different temperatures of seventeen reaction sintered and liquid phase sintered sialon. Fracture toughness, K_{1C} (SENB), values used in Table 4 were taken from a recent work /16/ of the present authors.

Out of the 17 cases, only in four (samples 3A, 11D, 13D and 17F) the difference between measured and predicted strength data were more than 25% whereas in the other thirteen cases the difference was less than 25% (Table 4). Three out of the four sialon samples, where mismatch between measured and predicted strength data was significant, were high temperature strength tested samples. In the cases of these three sialon samples (11D, 13D and 17F) the predicted strength was higher than the measured one. It is highly probable that in these three cases the flaw size was underestimated and actual failure is likely to have occurred due to multiple crack interaction effects /21/. The results of the present work indicate that if fracture toughness values are known, the fractographic methods can be successfully used to yield reliable estimates of strength in the temperature range 30-1200°C of reaction sintered and liquid phase sintered sialon samples.

4. SUMMARY AND CONCLUSIONS

(i) Out of the three different reaction sintered sialon products C, B and A, the last one had the best strength and Young's moduli characteristics in the temperature range 30-1400°C.

(ii) In the temperature range 30-1200°C, liquid phase sintered sialon D, synthesised with 5 wt.% of nitrogen rich liquid from the Y_2O_3-AlN-SiO_2 system, showed much improved strength and Young's moduli characteristics compared to sialon F, synthesised with 8 wt.% of silicate rich liquid from the MgO-SiO_2 system.

TABLE 4

Comparison of strength predicted fractographically and measured experimentally at different temperatures of sialon

Sample No.	Temp (°C)	Fracture toughness K_{1C}* (MPa . $m^{1/2}$)	Z	Y	Measured Flaw Size (μm)	Strength (MPa)	
						Measured	Predicted
1A	30	3.37	1.80	2	71	349	360
2A	30	3.20	1.15	2	21	349	402
3A	30	3.37	1.62	2	178	301	205
4A	30	3.37	1.58	2	98	290	269
5A	1200	3.36	1.05	2	34	345	303
6C	1200	3.33	1.58	2	103	224	259
7C	1200	3.33	1.00	2	278	91	100
8D	30	5.28	1.25	2	67	360	403
9D	800	5.24	1.14	2	48	398	431
10D	1000	5.14	1.00	2	72	327	303
11D	1000	6.05	1.20	2	71	284	431
12D	1200	4.58	1.58	2	280	217	216
13D	1200	6.17	1.42	2	158	214	349
14F	30	3.59	1.79	2	221	221	216
15F	900	3.60	1.58	2	188	210	207
16F	1100	3.00	1.58	2	202	170	167
17F	1100	2.10	1.58	1.77	36	221	312

* Measured by SENB technique (Ref. 16).

(iii) Under ambient condition, the Young's moduli of liquid phase sintered sialon samples (D, E and F) increased with decrease in average grain size.

(iv) At 30 and 1200°C in both reaction sintered sialon (A, B and C) and liquid phase sintered sialon (D and F), an improvement or degradation in strength was associated with corresponding improvement or degradation in their respective Young's moduli and fracture toughness (K_{1C}) values.

(v) In the cases of thirteen out of seventeen sialon samples studied, there was very god matching between fractographically predicted and experimentally measured strength data.

REFERENCES

1. WILLS R.R., STEWART R.W. and WIMMER J.M., "Fabrication of reaction sintered sialon". *J. Am. Ceram. Soc.*, **60**, 64-67, (1977).
2. MITOMO M., HASAGAWA Y., BANDO Y., WATANABE A. and SUZUKI H., "The strength of hot pressed beta-sialon". *J. Cer. Soc. Jap.*, **88**, 298-304, (1980).
3. MITOMO M., KARAMATA N. and INOMATA Y., "Fabrication of high strength beta-sialon by reaction sintering". *J. Mat. Sci.*, **14**, 2309-2316, (1979).

4. BRIGGS J., "Pressureless sintering of sialon ceramics". *Mater. Res. Bull.*, **12**, 1047-1055, (1977).
5. CAPALL D.S. and DUTTA S., "Effect of heating rate on density, microstructure and strength of Si_3N_4-6 wt.% Y_2O_3 and a β'-sialon". *Am. Ceram. Soc. Bull.*, **61**, 854-856, (1982).
6. DUTTA S., "Fabrication, microstructure and strength of sintered β'-Si_3N_4 solid solution". *Am. Ceram. Soc. Bull.*, **59**, 623-626, (1980).
7. LAYDEN, G.K., **Development of sialon materials.** Tech. Rept. No. R77-912184-21(1977), United Technologies Research Center, East Hartford, Connectient, USA.
8. LUMBY R.J., "Preparation, structure and properties of commercial sialons". *Cer. Eng. Sci. Proc.*, **3**, 50-66, (1982).
9. LARSEN D.C., ADAMS J.W., JOHNSON L.R., TEOTIA A.P.S. and HILL L.G., **Ceramic materials for advanced heat-engines, technical and economic evaluation.** Noyes Publications (1986), New Jersey, USA.
10. MUKHOPADHYAY A.K., CHAKRABORTY D. and MUKERJI J., "Fractorgraphic study of sintered Si_3N_4, Sialon and RBSN". *J. Mat. Sci. Lett.*, **6**, 1198-1200, (1987).
11. CHAKRABORTY D. and MUKHOPADHYAY A.K., "Creep of sintered silicon nitirde". *Ceramics International*, **15**, 237-245 (1989).
12. MUKHOPADHYAY A.K., "Study parameters influencing fracture toughness of silicon nitride and its composites". Ph.D. Thesis, Jadavpur University, (1987), Calcutta, India.
13. CHAKRABORTY D. and MUKHOPADHYAY A.K., "Creep of reaction sintered and liquid phase sintered sialon". **International Conference on Sintering of Multiphase Metal and Ceramic Systems**, New Delhi, India, (1989).
14. MUKHOPADHYAY A.K. and CHAKRABORTY D., "Influence of some parameters on strength and fracture toughness of reaction-bonded silicon nitride". *Trans. Ind. Ceram. Soc.*, **47**, 36-42, (1988).
15. CHAKRABORTY D. and MUKHOPADHYAY A.K., "High temperature Young's modulus of reaction bonded silicon nitride, liquid phase sintered silicon nitride and sialon". *Ceramics International*, **14**,, 127-132, (1988).
16. MUKHOPADHYAY A.K. and CHAKRABORTY D., "High temperature fracture toughness and fractographic study of reaction sintered and liquid phase sintered sialon". *Mater. Sci. Eng.*, **A104**, 215-222, (1988).
17. CHAKRABORTY D. and MUKHOPADHYAY A.K., "Fractography of silocon nitride and sialon ceramics". *Central Glass and Ceramic Rrsearch Institute Bulletin*, **34**, 59-69, (1987).
18. HAMPSHIRE S. and JACK K.H., "The Kinetics of densification and phase transformation of nitrogen ceramics". *Proc. Brit. Ceram. Soc.*, **31**, 37-49, (1981).
19. MUKHOPADHYAY A.K. and CHAKRABORTY D., "Critical evaluation of high temperature fracture toughness of sintered silicon nitride". **National Workshop on Advanced Ceramic Materials**, Calcutta, India, (1988).
20. GREEN D.J., "Fracture toughness/Young's modulus correlation for low density fibrous silica bodies", *J. Am. Ceram. Soc.*, **66**, 288- 292, (1983).
21. EVANS A.G. and TAPPIN G., "Effects of microstructure on the stress to propagate inherent flaws". *Proc. Brit. Ceram. Soc.*, **20**, 275-297, (1972).